Dragster: An Assimilative Tool for Satellite Drag Specification

Marcin D. Pilinski
University of Colorado at Boulder / Laboratory for Atmospheric and Space Physics, Boulder, CO 80303

Geoff Crowley
ASTRA LLC., Louisville, CO 80027

Matt Seaton
ASTRA LLC., Louisville, CO 80027

Eric Sutton
Space Weather Technology, Research, and Education Center, Boulder CO 80303

1. ABSTRACT SUMMARY

Satellite drag constitutes one of the largest uncertainties to orbit prediction below 1000 km altitudes. We describe recent developments in an assimilative scheme called Dragster. The goal of this ongoing work is to improve satellite drag specification in low earth orbit. The performance of the enhanced Dragster technique is compared with other models using both drag-derived and optical observations of the atmosphere.

2. INTRODUCTION

Much as aircraft are affected by the prevailing winds and weather conditions in which they fly, satellites are affected by the variability in density and motion of the near-earth space environment. Drastic changes in the neutral density of the thermosphere, caused by geomagnetic storms or other phenomena, result in some of the most significant perturbations of LEO satellite motions through drag on the satellite surfaces. This can lead to difficulties in accurately locating satellites, temporarily losing track of satellites, and errors when predicting collisions in space. As the population of satellites in Earth orbit grows, higher space-weather prediction accuracy is required for critical missions, such as accurate catalog maintenance, collision avoidance for manned and unmanned space flight.

The Dragster assimilative atmospheric tool was developed by ASTRA LLC. in conjunction with university and government partners to address this critical need. The main objective of the Dragster tool was to reduce conjunction analysis errors through better aerodynamic force modeling along the satellite orbit. Dragster assimilates orbital data from 70-100 LEO space objects into an ensemble of atmospheric models. Solar and geomagnetic forcing parameters are included in the state vector as they are critical to determining the atmospheric state. Currently, ASTRA LLC. is working with the University of Colorado, Boulder on several significant updates to the Dragster tool that will help build an enhanced, comprehensive, nowcast and forecast of the satellite drag environment.

To date, Dragster has primarily used two-line element (TLE) orbit data and empirical atmospheric models for its validation and testing. Recent developments have added the capability to assimilate orbital data based on special-perturbation (SP) orbit solutions which have higher-cadence and accuracy than TLE's. Furthermore, the ensemble management system has been upgraded to include multiple parallelized ensembles of Global Circulation Models (GCM's) running across an arbitrary number of processing cores and computers. Unlike empirical models of the atmosphere, the GCM's solve for the coupled fluid motions in the upper atmosphere providing a more spatially resolved picture of the satellite drag environment.

In this paper, we will first review the Dragster architecture and design. Next, we present validation results of the Dragster assimilation. As part of the validation, we compare the drag observed by a variety of satellites which were not used as part of the assimilation-dataset and whose perigee altitudes span a range from 200 km to 700 km. We also compare Dragster results with remote sensing observations of the atmosphere which are independent of satellite drag entirely.

3. OVERVIEW OF DRAGSTER

Dragster is a data assimilation scheme designed to evaluate the ingestion of General Perturbations (GP) and Special Perturbations (SP) data into empirical and general circulation models. Dragster uses a configurable ensemble of atmospheric models to estimate the covariance and calculate the Kalman gain. The top level procedure is illustrated by the flow diagram in Fig. 1. Unlike a classical Ensemble Kalman Filter, Dragster estimates covariance and forms state estimates iteratively at each assimilation time window (orange parts of Fig. 1 in the lower left corner of the flow diagram) giving it some similarities to a batch processing estimator.

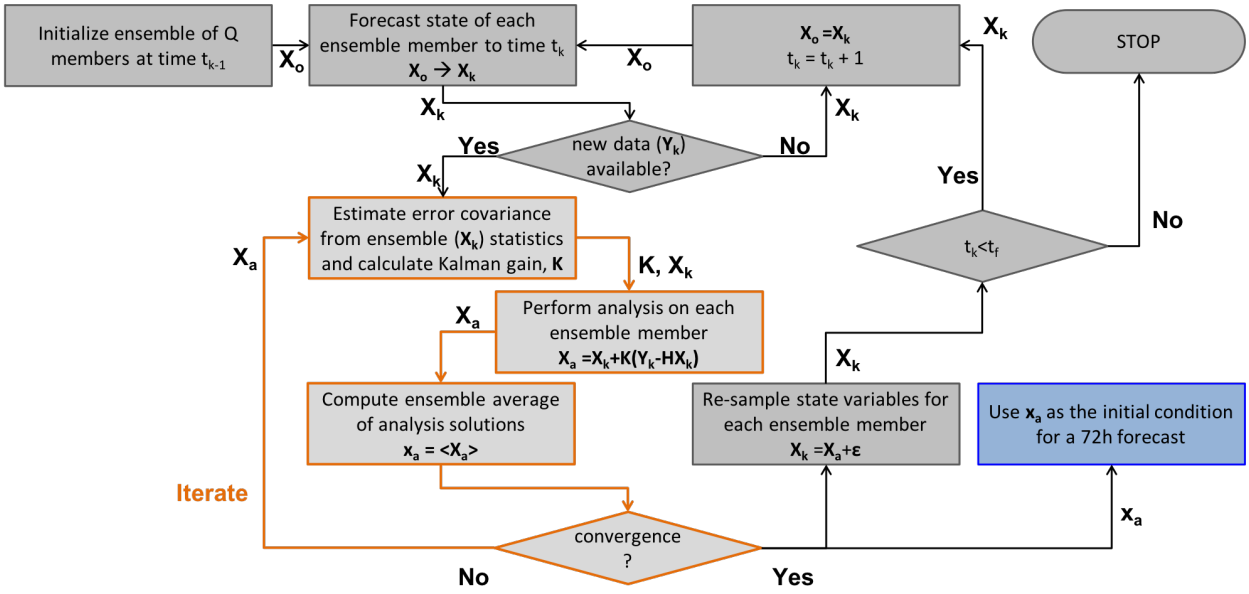

Fig. 1. Process flow diagram for the Dragster assimilative tool.

The software is designed such that atmospheric models making up the ensemble can be switched out for evaluation purposes. At the time of writing, Dragster has been tested with ensembles of NRLMSISE-00 [REF] atmospheric models as well as TIE-GCM2.0 [REF] global circulation model (GCM).

Each ensemble state at time *tk*, $\mathbf{X}_{tk}$, is composed of the state solutions for the ensemble members $\mathbf{x}_{tk,i}$, which contain an array including both model field factors $x_{tk,i,j}$ and model forcing factors $F_{tk,i,j}$.

$$\mathbf{X}_{t_k}^f = \left[\mathbf{x}_{t_k,1}^f \quad \mathbf{x}_{t_k,2}^f \quad \ldots \quad \mathbf{x}_{t_k,q}^f\right] \quad \text{where} \quad \mathbf{x}_i^f = \begin{bmatrix} x_{t_k,i,1}^f \\ \vdots \\ x_{t_k,i,N}^f \end{bmatrix}$$

$$x_{t_k,i,j}^f = \begin{cases} x_{t_k,i,j} & \text{model field factors} \\ F_{t_k,i,j}\left(x_{t_k,i,j}\right) & \text{model forcing} \end{cases} \quad (j = 1 \ldots N)$$

Model forcing includes solar and geomagnetic forcing parameters. For the purposes of this paper, these will be represented by F10.7 solar EUV proxy and the Ap geomagnetic index. Model field factors are corrections to the modeled atmospheric state for each ensemble member. The field factors are specified for a pre-defined local-time, latitude, and altitude grid.

4. INPUT DATA

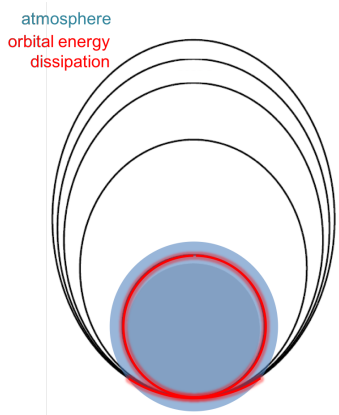

Fig. 2. Illustration of how satellite drag can contain various levels of localization regarding the atmospheric state.

Dragster works by assimilating the observed drag from 50-100 satellites. The procedure for processing orbital data for Dragster is described by Pilinski et al. [8]. Fig. 2 shows orbits with various levels of eccentricity and where these orbits might intersect the thickest part of the upper atmosphere (red). In the highly elliptical cases, the majority of satellite drag is confined to a section of the atmosphere. When interpreting this drag as an "effective density" for assimilation into Dragster, the information can be described to that section of the atmosphere only. As an orbit becomes more circular, the information contained in the satellite drag observation (orbit change) is integrated over geographically wider regions. However, because the atmosphere is asymmetric dayside densities are several times higher than nightside, some localization always exists. This allows for the recovery of atmospheric density fields at a variety of local times, altitudes, and latitudes without having to rely one highly resolved measurements such as accelerometers or mass spectrometers.

The example results that will be shown in this paper use orbital drag products derived from two line elements (TLE's) for 73 satellites, spanning 180-1000 km in perigee altitudes. They are processed into densities using the method presented by Picone et al. [9]. Drag derived from SP orbit fits has also been tested in Dragster. GRACE accelerometer data processed by Eric Sutton is used as a validation dataset (was not assimilated by Dragster).

Another source of validation data are solar occultation measurements made by the Lyra instrument on Proba II (see Fig. 3). Here, atmospheric number densities are derived from observations of the occulting sun from a LEO spacecraft. The density retrieval integrates the solar disk over a reference atmosphere to find a column density by examining the extinction of extreme ultraviolet light (EUV). Because EUV varies over the solar disk, disk images need to be incorporated into the retrieval (EUV images provided by SWAP Telescope [10]). A full description and validation of these retrievals is described in Thiemann et al. 2017 [11]. Note that solar occultations necessarily limit the location of the observed profiles to dawn and dusk local times.

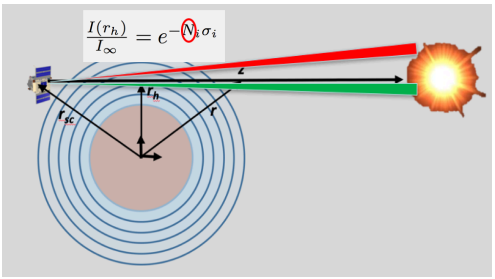

Fig. 3. Retrieving atmospheric density profiles from solar occultations.

5. RESULTS

The results below are based on a model run with ninety NRLMSISE-00 model ensemble members. Approximately one day assimilation windows were used to ingest the data over the span of 6 months from November 2015 to April 10, 2016. The estimated forcing parameters are shown in Fig. 4 and compared to the observed forcing. Note that any discrepancy between the observed and estimated forcing can be due to the inability of the observed index or proxy to capture the energy input into the atmosphere as well as the inability of the Dragster estimation to fully distinguish between solar EUV and geomagnetic energy inputs.

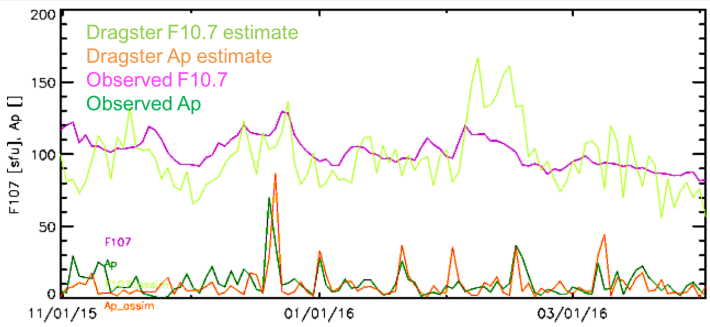

Fig. 4. Observed and estimated forcing parameters.

The density residual results are summarized as a function of altitude in Fig. 5. The panels show the errors for each assimilation satellite with horizontal bars representing the standard deviation of the relative observation- model difference. The points represent the average of the observation-model difference i.e. the bias associated with that satellite. The left panel shows the observed-model errors for the NRLMSISE-00 background model over the span of the 6-month test period. The right panel contains the errors after Dragster assimilation. Note the significant reduction of bias and standard deviation after the assimilation.

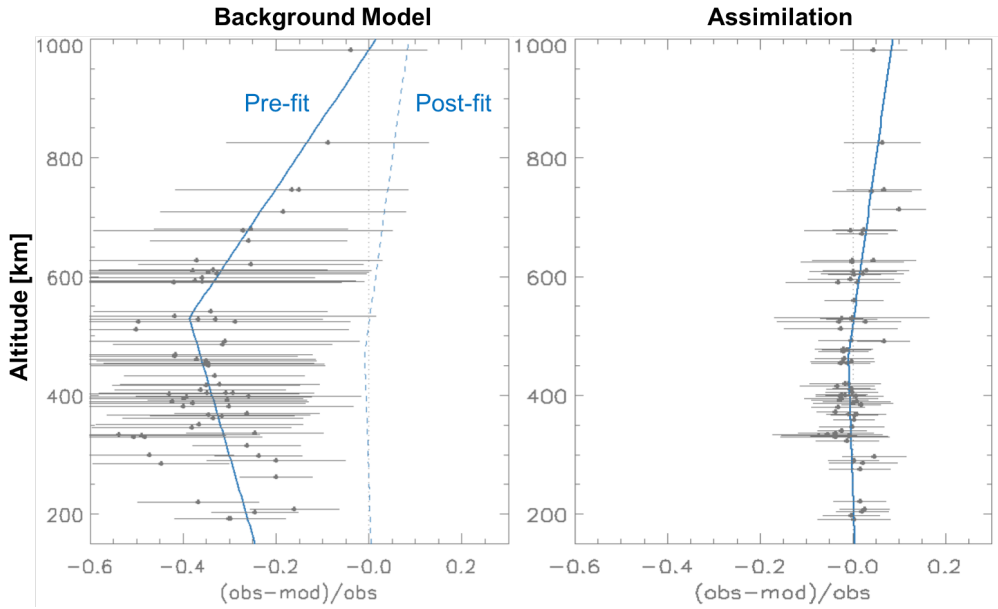

Fig. 5. Altitude profiles of atmospheric errors as standard deviation (horizontal lines) and biases (dots) before assimilation on the left and after assimilation on the right.

The results should also be compared with atmospheric measurements which were not assimilated into Dragster. First we compare select dawn and dusk density profiles measured by Lyra with the NRLMSISE-00 model as well as with the Dragster number densities (Fig. 6 and Fig. 7). The Lyra data is shown as the lower and upper bound of estimated densities form the occultation retrieval. The Dragster results are shown in red and the NRLMSISE-00 results in blue.

In almost all cases the Dragster altitude profile matches the Lyra retrievals more closely than the NRLMSISE-00 background model.

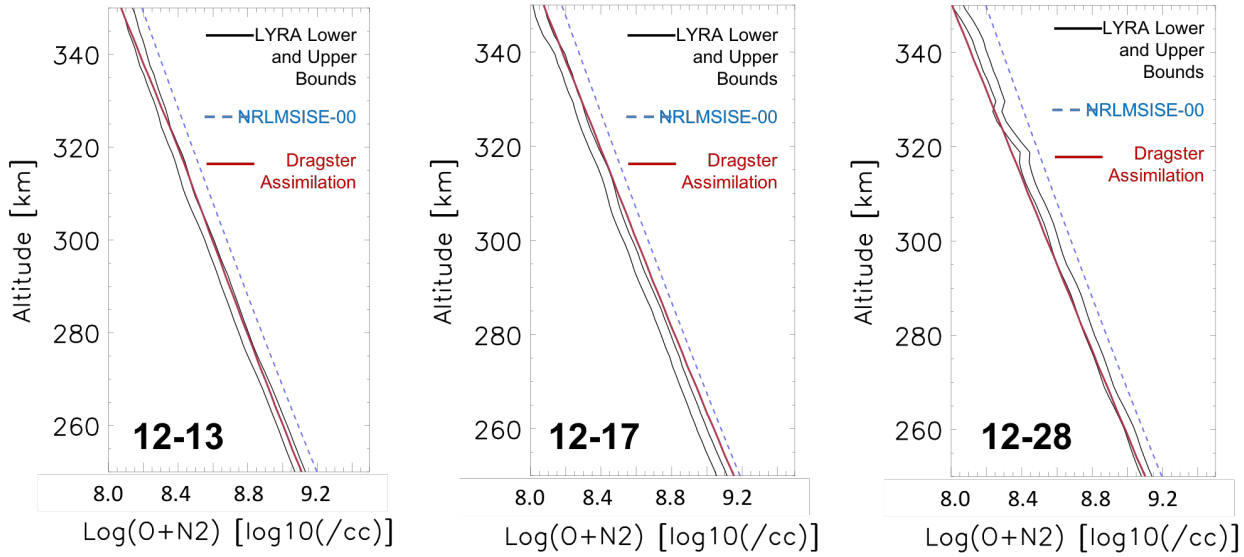

Fig. 6. Dawn occultation profiles for select dates.

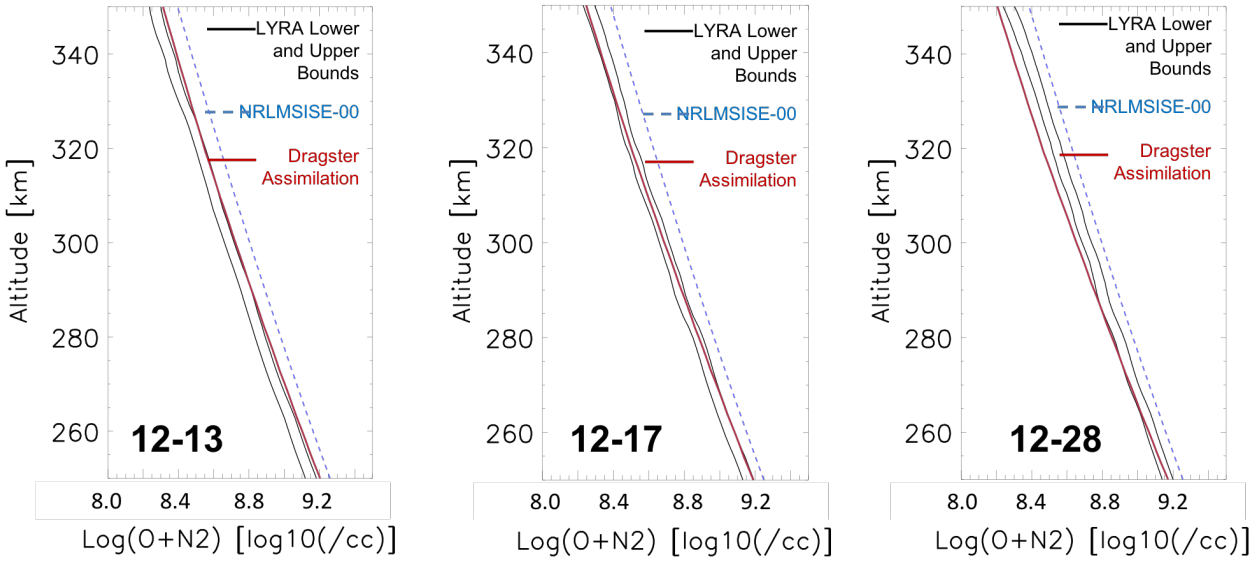

Fig. 7. Dusk occultation profiles for select dates.

Daily Lyra retrievals can also be summarized as densities at a fixed altitude (Fig. 8). The time series view shows that the assimilated densities match the Lyra measurements more closely than the background model (blue). The bottom panel shows contextual information including solar and geomagnetic forcing as well as the latitude at which the retrieval is made.

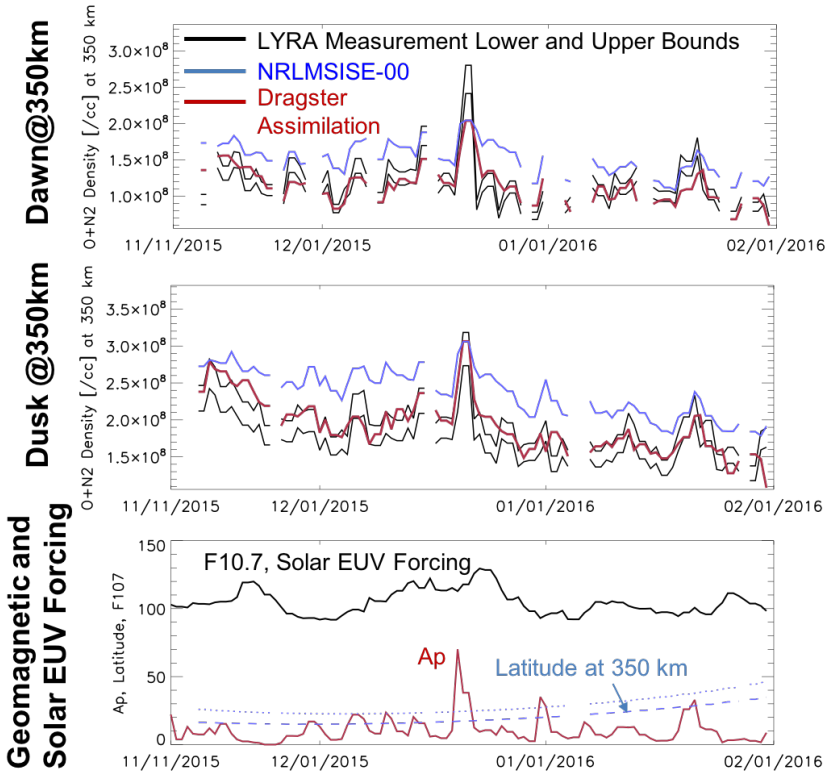

Fig. 8. Lyra, Dragster, and NRLMSISE-00 densities at 350 km altitudes. The top panel corresponds to Dawn densities, the middle panel to Dusk densities, and the bottom panel shows the solar and geomagnetic forcing as well as the latitude of the Lyra tangent-point.

Another source of validation data is the GRACE satellite accelerometer. This instrument measures densities along the GRACE orbit at 3-degree resolution. An example of two orbits of data is shown in Fig. 9.

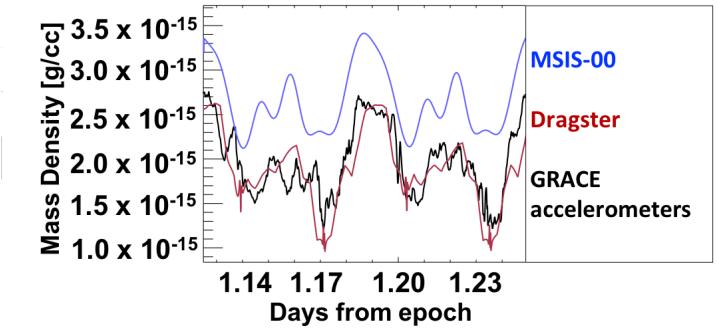

Fig. 9. GRACE accelerometers (black) along with Dragster (red) and NRLMISE-00 (blue) densities.

Note that Dragster improves not only the mean atmospheric state over the course of the orbits, but also the variations within each orbit which correspond to the latitudinal and local time structure of the atmosphere. The accelerometer data can be combined into daily-average orbits by averaging the orbital densities at each time since the ascending node passage. Examples of this are shown in Fig. 10. In general, Dragster can be seen to add sub-orbital structure to the atmosphere and improve the data-model bias. The standard deviation of the differences between Dragster and the GRACE measurements taken at the cadence of the measurements is approximately half of the standard deviation between GRACE and the background density model.

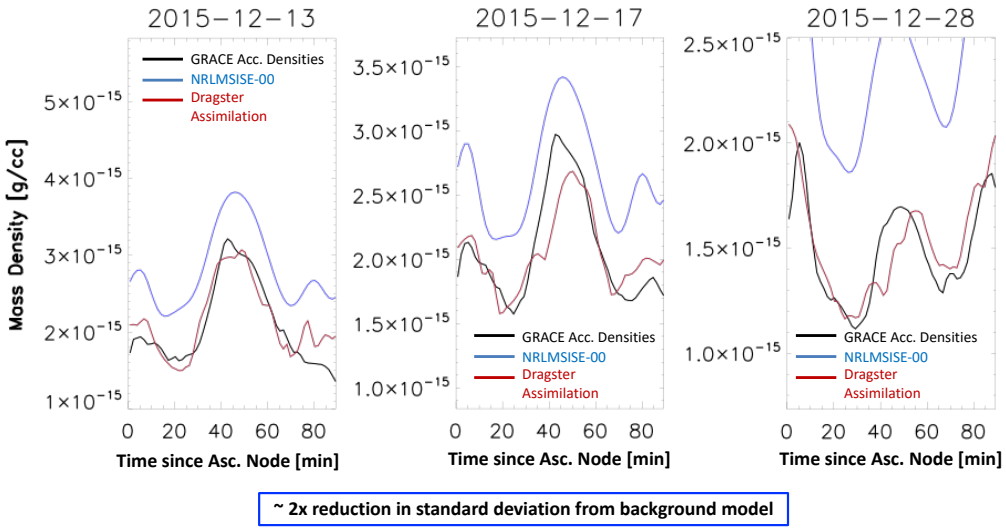

Fig 10: Daily average orbits show the average variation of density along each orbit for three select days.

6. CONCLUSIONS

The analysis presented in this paper indicates that significant post-fit error reduction over the background model is achieved using Dragster. Comparisons with an independent dataset, such as GRACE, indicate that Dragster can improve the density specification over NRLMSISE-00 by a factor of ~2x. Comparison with Lyra occultations indicates that assimilating orbit-derived drag products can also improve the altitude structure of the assimilated atmosphere. These are promising results since only coarse TLE data was assimilated and an empirical model background was used. Ongoing work has already tested the functionality to assimilate information from special perturbation orbit products. Validation efforts continue on this front to quantify the improvement in density specification associated with this.

7. ACKNOWLEDGEMENTS

This work has been supported by Air Force STTR contract FA9453-14-C-0061. We thank the sponsor for their support.

8. REFERENCES

[1] Bruinsma, S. L., and J. M. Forbes (2007), Storm-Time Equatorial Density Enhancements Observed by CHAMP and GRACE, J. Spacecraft and Rockets, Vol. 44, No. 6, doi: 10.2514/1.28134.

[2] Doornbos E. (2011). Thermospheric Density and Wind Determination from Satellite Dynamics. PhD thesis, Delft University of Technology.

[3] Pilinski, M. D. and B. Argrow (2013a), Aerodynamic analysis based on CHAMP satellite lift-to-drag measurements, J. Spacecraft and Rockets, doi: 10.2514/1.A32394.

[4] Bowman B. R. and S. Hrncir (2007). Drag Coefficient Variability at 100-300 km from the Orbit Decay Analyses of Rocket Bodies. In AAS/AIAA Astrodynamics Specialist Conference, number AAS 07-262. AAS/AIAA.

[5] Pilinski M. D., B. M. Argrow, S. E. Palo, B. R. Bowman (2013b), Semi-Empirical Satellite Accommodation Model for Spherical and Randomly Tumbling Objects, Journal of Spacecraft and Rockets, Vol. 50, pp. 556-571, doi: 10.2514/1.A32348 .

[6] Crowley, G., Pilinski, M., and Azeem, I. (2012), Tutorial: The Neutral Atmosphere and the Satellite Drag Environment, AAS 12-035, 145-161.

[7] Sutton, E. K., R. S. Nerem, and J. M. Forbes (2007), Density and winds in the thermosphere deduced from accelerometer data, J. Spacecraft and Rockets, 44(6), 1210, doi:10.2514/1.28641.

[7] Shim, J-S, M. Kuznetsova, L. Rastaetter, M. Hesse, D. Bilitza, M. Burala, M. Codrescu, B. Emery, B. Foster, T. Fuller-Rowell, J. Huba, A. J. Mannucci, X. Pi, A. Ridley, Ludger Scherliess, Robert W. Schunk, P. Stephens, D. C. Thompson, Lie Zhu, D. Anderson, J. L. Chau, Jan J. Sojka, and B. Rideout (2011), CEDAR Electrodynamics Thermosphere Ionosphere (ETI) Challenge for Systematic Assessment of Ionosphere/Thermosphere Models 1: NmF2, hmF2, and Vertical Drift Using Ground Based Observations, Space Weather Journal, Vol. 9, S12003, doi:10.1029/2011SW000727.

[8] Pilinski, M.D, G. Crowley, E. Sutton, M. Codrescu, Improved Orbital Determination and Forecasts with an Assimilative Tool for Satellite Drag Specification, Conference Proceedings, 50th Advanced Maui Optical and Space Surveillance Technologies, Maui, HI, 20-23 September, 2016

[9] Picone, J. M., J. T. Emmert, and J. L. Lean (2005), Thermospheric densities derived from spacecraft orbits: Accurate processing of two-line element sets, J. Geophys. Res., 110, A03301

[10] Halain, JP., Berghmans, D., Seaton, D.B. et al. Sol Phys (2013) 286: 67. https://doi.org/10.1007/s11207-012-0183-6

[11] Thiemann, E. M. B., Dominique, M., Pilinski, M. D., & Eparvier, F. G. (2017). Vertical thermospheric density profiles from EUV solar Occultations made by PROBA2 LYRA for solar cycle 24. Space Weather, 15, 1649–1660. https://doi.org/10.1002/2017SW001719